Bioturbation experiments in the Venice Lagoon

C. Mugnai[1,*], M. Gerino[2], M. Frignani[1], S. Sauvage[2] & L. G. Bellucci[1]
[1]*Istituto di Geologia Marina del CNR, Bologna, Italy*
[2]*Centre d'Ecologie des Systèmes Aquatiques Continentaux, Toulouse, France*
[*]*Present address: ICRAM c/o CIBM, Viale N. Sauro 4, 57128 Livorno, Italy*
Tel.: +39-0586-260201. Fax: +39-0586-809149. E-mail: ilmugno@tin.it

Key words: bioturbation, luminophores, sediment mixing, modeling, Venice Lagoon

Abstract

Short experiments (14–21 days) were carried out during autumn 1998 and spring 1999 at one selected site of the Venice Lagoon to measure bioturbation activities and mixing rates, as well as to obtain quantitative information on benthos functionality. Fluorescent sediment particles (luminophores, 63–350 μm) were introduced as pulse inputs at the sediment surface. The concentration–depth profiles of the tracer were simulated with a new advection–diffusion–non local model applied under non-steady state conditions. This allowed the quantification of the mixing parameters associated with different mechanisms: biodiffusion (D_b), bioadvection (W) and non-local mixing (Ke, z_1, z_2). A parameter RS (removed sediment) was also calculated to account for the flux of sediment due to non-local transport. Results show that bioturbation was dominated by biodiffusion in autumn and by bioadvection in spring. Mean mixing parameters Db, W, and RS changed from 3.09 to 0.87 $cm^2\ y^{-1}$, from 0.93 to 15.50 y^{-1} and from 5.85 to 7.79 $g\ cm^{-2}\ y^{-1}$, respectively.

Introduction

Bioturbation is defined as the process of sediment mixing that results from macrofauna burrowing, feeding, and reworking within the surficial sediment. This process has profound effects on both early diagenesis and preservation of sediment records. In fact, the rates of oxygen penetration and organic matter decomposition, the dissolution of biogenic components such as $CaCO_3$ and SiO_2, and the pore water concentrations of nearly all dissolved species are affected by bioturbation as a function of its intensity (Berner, 1980; Aller, 1982; Wheatcroft et al., 1990, 1992). Furthermore, the displacement of interstitial fluids, the increase of sediment surface in contact with bottom water, and irrigation enhance the exchange of dissolved species at the sediment–water interface. In addition, the displacement of particles and particle reactive species blurs or destroys the sediment record, i.e., the information that sediment can store in their strata. Therefore, a better understanding of bioturbation in its mechanisms, rates, and effects is important for a wide range of disciplines.

In the past, biogeochemists have approached bioturbation through simplified models based on the analogy with diffusion (e.g., Wheatcroft et al., 1990). The community-wide mixing rates were obtained by measuring the vertical concentration profiles of various tracers and fitting theoretical profiles to the observed gradients. The calculated biodiffusivity (D_b), which integrates all bioturbation activities over a sufficiently long time, cannot explain short time-scale effects. Among these, a tracer distribution with a maximum at the surface, followed by a sharp decrease with depth, is typically generated by biodiffusive mixing (Guinasso & Schink, 1975; Cochran, 1985; Wheatcroft et al., 1990). This mixing is produced by organisms that move sediment particles in a random manner over short distances. On the contrary, subsurficial peaks are generated by vertical transfer of the tracers to depth caused by two independent processes: bioadvection (Fisher et al., 1980) and non local transport (Boudreau, 1986). Bioadvective transport is generated by head-down oriented organisms called 'conveyor-belt species' that cause an active transport of sediment trough their gut from the ingestion zone located at depth in the sediment to the sediment surface (Fisher et al., 1980; Rice, 1986; Gerino et al., 1994). Their effect on a tracer profile is similar to that due to a high accumulation rate. In turn, non-local

mixing is caused by two mechanisms: one is due to the egestion of fecal pellet at depth by surface deposit feeders denominated 'inverse conveyors', whereas the other, called 'regeneration', supplies fresh material that mechanically drops into burrows from the interface to depth (Smith et al, 1986/87; Gardner et al., 1987; François et al., 1997).

Several models have been proposed to simulate bioturbation mechanisms different from diffusion (Fisher et al., 1980; Smith et al., 1986/87; Gardner et al., 1987; Boudreau, 1997; Gerino et al., 1994, 1998). In particular, Gerino et al. (1998) used a particle transport model containing both diffusive and advective terms to simulate the depth distribution of the pulse input of a conservative tracer. An evolution of this model, which is able to account for non local mixing, is used in this paper. In the present study, an experiment was carried out to obtain information on bioturbation mechanisms and rates in a shallow environment of the Venice Lagoon. This site was selected because it is not disturbed by marine traffic and by the illegal clam fishing that affects a great part of the lagoon.

Materials and methods

Figure 1 shows the study area and the experimental site. G is located at 0.5 m depth in the central part of the Palude di Cona. It corresponds to a typical shallow water environment with estuarine characteristics that receives the discharge of the Dese river, one of the main freshwater suppliers to the lagoon (Zonta et al., 1994).

The experimental procedure, based on the use of dyed sediment particles called luminophores, was described in detail by Gerino (1990) and Gerino et al. (1994). Experiments were carried out in autumn 1998 and in spring 1999. At the experimental site, three open PVC tubes (25 cm long, 12.2 cm i.d.) were inserted into the sediment and a thin frozen mud cake (0.5 cm thick), containing 2 g of both pink and green tracer (63–125 μm), was set at the sediment surface thus simulating a pulse input. One control core with defaunated sediment was set in similar conditions. The tubes were carefully retrieved after 15 days in autumn and 21 days in spring, quickly transferred to the laboratory and subsampled at 0.5–5 cm intervals. Luminophores were counted with a microscope under UV light, and counts were converted into weight units using the number of particles per mass of luminophores in a given size fraction divided by the weight of sediment. Furthermore, the tracer profile in each core was normalized against its inventory.

Results and discussion

The tracer vertical distributions (Fig. 2) show evident penetration of luminophores in the experimental cores. On the contrary, the tracer remained confined at the surface in the control cores, even if in spring there is an expansion of the surficial peak down to a depth of 2 cm, thus excluding physical disturbance. However, the three depth-distributions obtained from each experiment are never identical, in that they exhibit multiple tracer peaks at different depth in the subsurface zone. In particular, the autumn profiles G(a) show an average penetration of 8 ± 3 cm (median $\pm$ range of variation, n = 3), with the highest concentration close to the surface. $G(a)_1$ shows three well-defined subsurface peaks (Fig. 2), whereas tracer accumulations are less marked and closer to the surface in $G(a)_2$ and $G(a)_3$. In spring cores, especially $G(s)_1$ and $G(s)_3$, the maximum concentrations are located immediately below the sediment surface. These distributions account for the presence of advective transport. The heterogeneity of biological transport processes in replicate cores is probably an effect of the non-homogeneous horizontal macrofauna distribution at the decimetric scale of the cores.

To estimate bioturbation parameters, the profiles were simulated using the bioadvection–biodiffusion–non local model in non-steady-state conditions. This model was developed by adding a non-local component to the regular diffusion advection model (Officer & Lynch, 1982, Gerino et al., 1994, 1998). The non-local mixing is modeled such as a removal function that determines the fraction of tracer removed from the surface within the particle collection zone, and an injection function that simulates the displacement of this material into the deposition zone. Since the experiments were conducted over a very short time period, and advection was not recorded in the control cores, the sedimentation rate is not taken into account in the model. The basic equation is:

$$\frac{\partial C(z,t)}{\partial t} = D_{\mathrm{b}} \frac{\partial^2 C(z,t)}{\partial z^2} - W \frac{\partial C(z,t)}{\partial z} + K(z,t) - R(z,t), \qquad (1)$$

where C is the normalized tracer concentration, t is the time (*years*), z is the depth (cm) positive down-

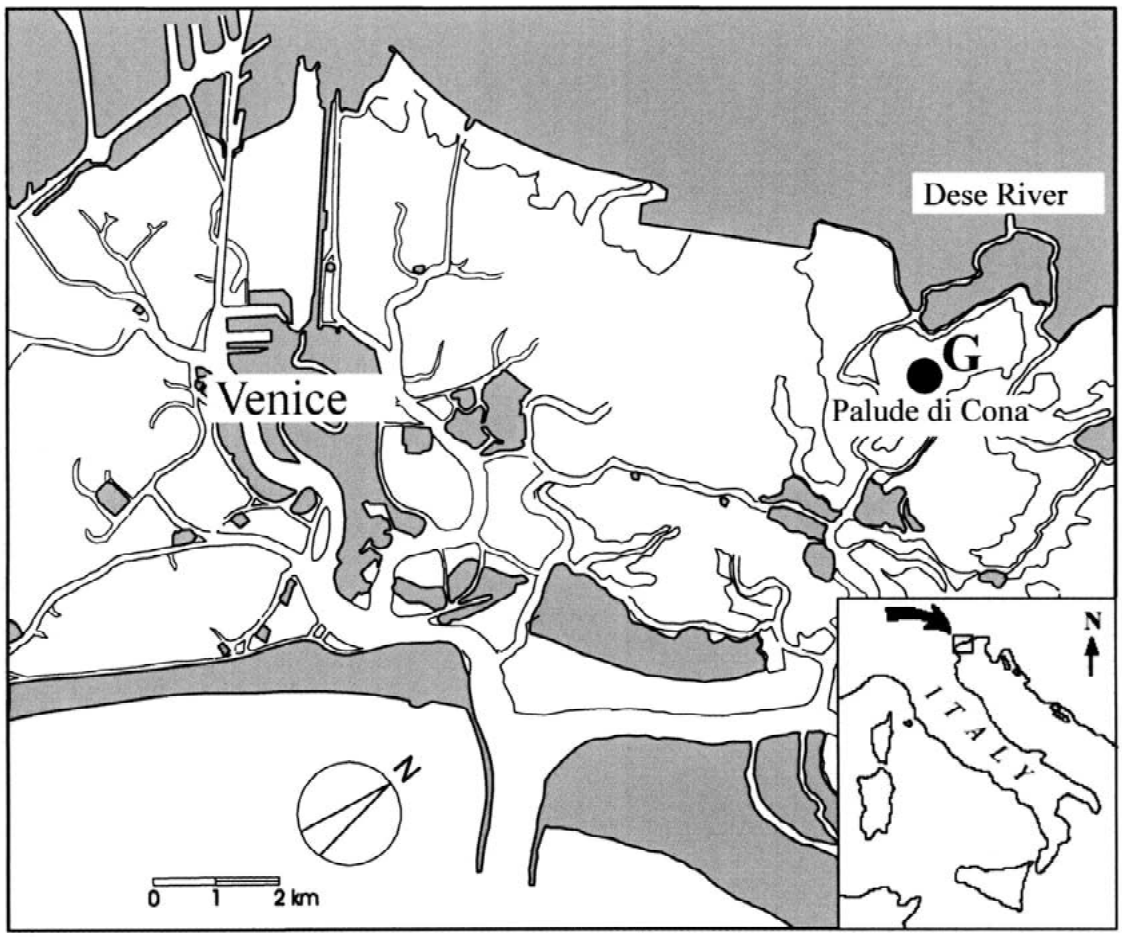

Figure 1. Study area and experimental site.

ward, D_b is the biodiffusive mixing rate ($cm^2\ y^{-1}$), W is the bioadvective transport rate ($cm\ y^{-1}$), and R is the removal function that determines the fraction of tracer ($g\ cm^{-3}\ y^{-1}$) removed from the surface. This quantity of tracer is collected at the sediment surface by inverse conveyor or lost from the sediment surface by passively falling into the burrow. K is the injection function of the non-local transport that simulates tracer inputs ($g\ cm^{-3}\ y^{-1}$) into the injection zone of the sediment column and Ke is a constant parameter (y^{-1}) estimated from the model. The depths z_1 and z_2 represent the upper and lower limits of the injection zone respectively. The non-local transport is thus quantified by a flux of sediment 'removed from the surface', called Removed Sediment (RS, $g\ cm^{-2}\ y^{-1}$). Knowing that sediment was removed from a marked mud cake with a thickness of 0.5 cm, surface S (cm^2), density d ($g\ cm^{-3}$) and volume V (cm^3), RS can be expressed as a function of Ke (y^{-1}) that is RS = Ke (V/S) d. A parameter τ=0.5/W_{max} is introduced to account for the time during which the tracer is still at the top 0.5 cm of surface sediment and limits the period available for non-local transport. In this case:

$$R(z,t) = \begin{cases} 0 \text{ for z} > 0.5 \text{ or } t > \tau \\ k(z,t)\dfrac{z_2 - z_1}{0.5} \text{ for } z < 0.5 \text{ and } t < \tau \end{cases}$$

$$K(z,t) = \begin{cases} \text{Ke for } z \in [z_1, z_2] \\ 0 \text{ for } z \notin [z_1, z_2] \end{cases}$$

with model initial conditions

$$C(z, t = 0) = 1 \text{ for } z \in [0, 0.5]$$
$$C(z, t = 0) = 0 \text{ for } z > 0.5$$

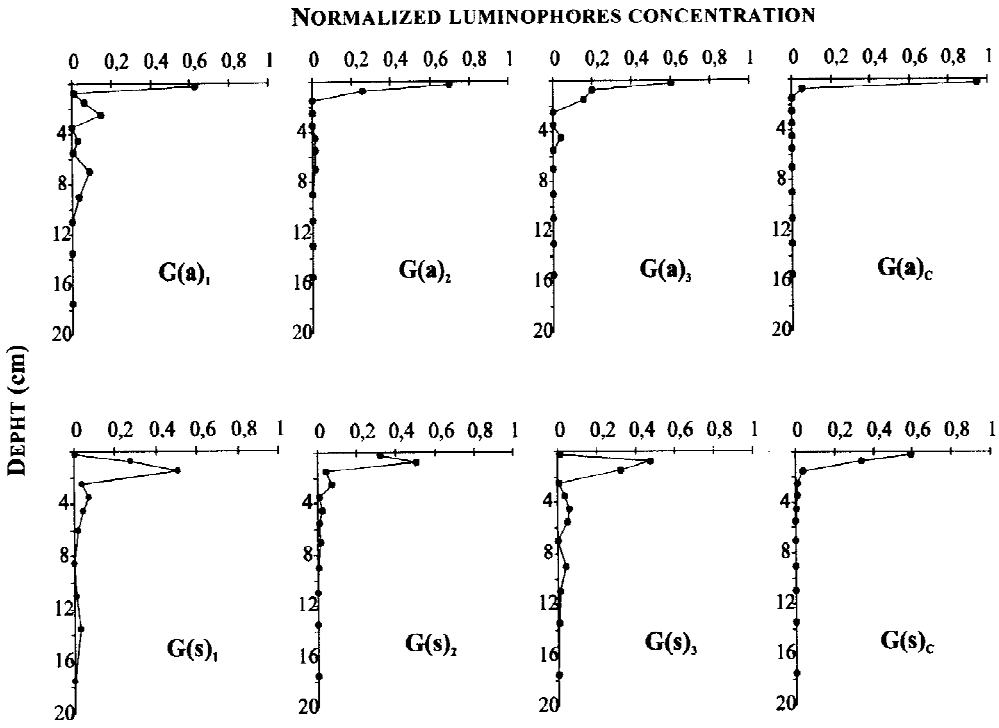

Figure 2. Concentration-depth profiles of luminophores in sediments. $G(a)_1$, $G(a)_2$, $G(a)_3$ and $G(s)_1$, $G(s)_2$, $G(s)_3$ are the experimental replicates obtained in autumn and in spring, respectively; $G(a)_c$ and $G(s)_c$ are the defaunated control cores. Values are normalized against total inventories.

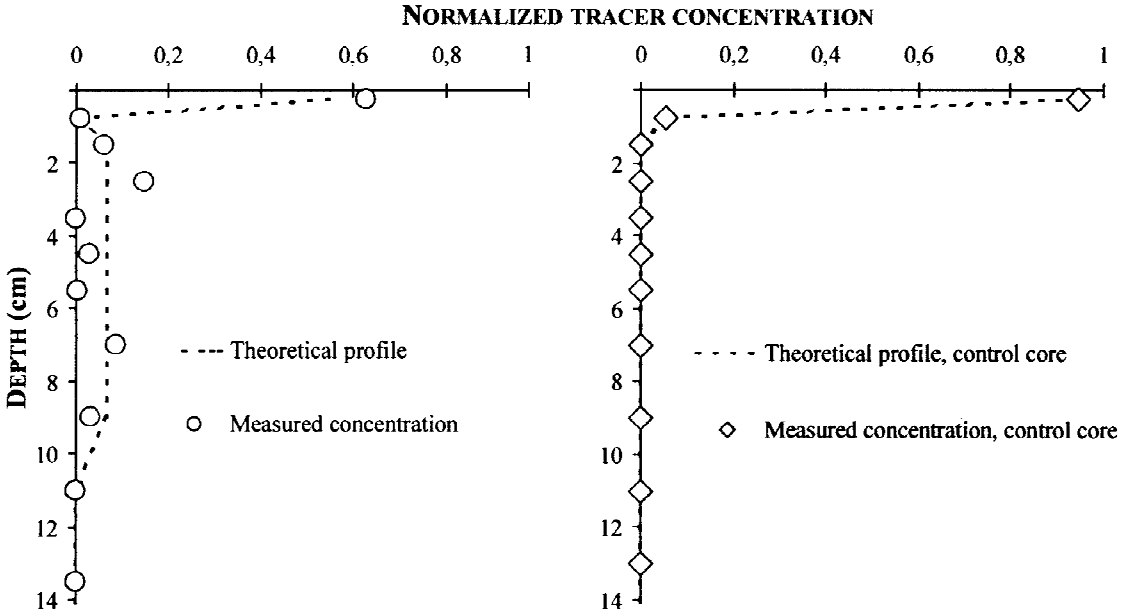

Figure 3. Best-fitting of the experimental profile $G(a)_1$ (core with fauna at site G during autumn 1998) with a theoretical profile. The best-fitting of the corresponding control (core without fauna at site G during autumn 1998) is also shown.

and boundary conditions

$$C(z \to +\infty, t) = 0$$

$$WC_{(z=0,t)} - D_{\mathrm{b}} \frac{\partial C}{\partial z} \,]_{z=0,t} = 0$$

an analytical solution is provided by Officier & Lynch (1982):

$$C(z,t) = \frac{1}{\sqrt{\Pi D_{\mathrm{b}} t}} \exp\left[-\frac{(z-Wt)^2}{4D_{\mathrm{b}}t}\right] - \frac{W}{2D_{\mathrm{b}}} \exp\left(\frac{Wz}{D_{\mathrm{b}}} erfc \frac{z+Wt}{\sqrt{4D_{\mathrm{b}}t}} - Ret + Ket\right.$$

with

$$\mathrm{Re} = Ke \frac{Z_2 - Z_1}{0.5} \tag{2}$$

Since experimental time remains relatively short compared to advection velocities, and because the highest tracer concentrations remain very close to the surface, it is assumed that the initial tracer impulse has never migrated down to the limit depth where the organisms ingest food and sediment (Fischer et al., 1980) *via* bioadvective processes. The model allows the calculation of the theoretical tracer concentration given suitable values of the parameters D_{b}, W, z_1, z_2, Ke, τ. These parameters are selected from profiles that produce the best fit with the experimental data using the least square method. When two or three subsurficial peaks were present, the upper tracer profile was assigned to bioadvective and/or biodiffusive processes, and other deeper tracers accumulations were taken into account as due to non local processes. The total theoretical profile is the sum of the theoretical sub-profile concentrations. Figure 3 shows an example through the bestfitting of the tracer depth-distribution in core $G(a)_1$.

Table 1 shows the values of D_{b}, W, Ke, z_1, z_2, and RS estimated from each experimental profile. Coefficients are comparable with those reported in the literature (Aller & Cochran, 1976; Benninger et al., 1979; Clifton, 1991; Gerino et al., 1994; Gerino et al., 1998) and in most cases obtained with the same method in environments with a morphology similar to that of the Venice Lagoon. D. Prevedelli (pers. com.) studied the macrofaunal density and composition at the experimental site in the two seasons. Results suggest that oligochaeta and the polychaeta *Hediste diversicolor* and *Streblospio shrubsolii* are the main responsible of non-local mixing. On the other hand, the seasonal differences of W could be attributed to several factors. In particular, the increased temperature could have enhanced biological activities or induced changes in the functional composition of the benthic community.

Conclusions

The following conclusions can be drawn: (1) the luminophores penetrated into the sediments only due to the activity of benthic organisms in that physical processes were not effective, as demonstrated by control cores; (2) the short time scale of the experiments and the use of the model allowed a clear discrimination and quantification of the diffusive, advective, and non-local processes under realistic *in situ* conditions. In spite of that, 2–3 weeks were not sufficient for the tracer to reach the depth of maximum ingestion, since the advective subsurficial peaks remain well defined; (3) the polychaeta *H. diversicolor* and *S. shrubsolii* are probably the major responsible of the non local mixing associated with deep tracer peaks; and (4) repeated experiments evidence a greater importance of bioadvective processes during spring than during autumn. This change might be attributed to several factors like temperature, macroinvertebrate community composition, or organic matter content. Identification of environmental factors controlling bioadvection should be further considered in situ or in laboratory experiments. In a future prospective, the inclusion of sedimentation in the bioturbation model will let us to simulate the formation of the sediment record. This will enable to make provision for the effects of changes of the contaminant inputs, very important in deciding any monitoring program.

Acknowledgements

Funds for this research were provided by the 'Project 2023' founded by the Ministry of Public Works through the Magistrato alle Acque of Venice and the Consorzio Venezia Nuova. This is contribution No. 1296 from the Istituto di Geologia Marina, Bologna (Italy).

Table 1. Bioturbation coefficients and RS values from model simulations. D_b; biodiffusive mixing rate; *W*; bioadvective mixing rate; *Ke*; downward transport of tracer displaced by 'non-local mixing'; z_1, z_2; upper and lower limits of the 'non-local mixing' zone; RS; removed sediment from the surface layer by non local transport, expressed per unit area of sediment–water interface. G(a) and G(s) represent average coefficients (mean ± confidence limit, $n = 3$, $p < 0.05$) for each season (a = autumn and s = spring). $G(a)_c$ and $G(s)_c$ are control core coefficients. These last values are given for information and do not enter in the calculation of average coefficients.

Site	D_b ($cm^2\ y^{-1}$)	*W* ($cm\ y^{-1}$)	*Ke* (y^{-1})	z_1 (cm)	z_2 (cm)	RS ($g\ cm^{-2}\ y^{-1}$)
$G(a)_1$	0.1	2.1	58.4	1	9	18.7
$G(a)_2$	3.2	0.2	7.3	4	7	2.3
$G(a)_3$	6	0.5	7.3	4	5	2.3
$G(a)_C$	1.1	0.3	0	0	0	0
G(a)	3.09 ± 3.36	0.93 ± 1.16	24.33 ± 33.38	3.00 ± 1.96	7.00 ± 2.26	7.79 ± 10.68
$G(s)_1$	0.5	19.8	14.6	2	5	4.7
$G(s)_2$	1.2	8.7	14.6	2	7	4.7
$G(s)_3$	0.9	18	25.5	3	10	8.2
$G(s)_C$	3.9	0	0	0	0	0
G(s)	0.87 ± 0.4	15.50 ± 6.74	18.25± 7.15	2.33 ± 0.65	7.33 ± 2.85	5.85 ± 2.30

References

Aller, R. C. & J. K. Cochran, 1976. $^{234}Th/^{238}U$ Disequilibrium in near-shore sediment: particle reworking and diagenetic time scales. Earth Planet. Sci. Lett. 29: 37–50.

Aller, R. C., 1982. The effects of macrobenthos on chemical properties of marine sediment and overlying water. In: McCall & M. J. S. Tevesz (eds), Animal–Sediment Relations, Plenum Press, New York: 53–102.

Benninger, L. K., R. C. Aller, J. K. Cochran & K. K. Turekian, 1979. Effects of biological sediment mixing on the ^{210}Pb chronology and trace metal distribution in a Long Island Sound sediment core. Earth Planet. Sc. Lett. 43: 241–259.

Berner, R. A., 1980. Early Diagenesis. A Theoretical Approach. Princeton University press, Princeton (N.J), 241 pp.

Boudreau, B. P., 1986. Mathematics of tracer mixing in sediments: II Non local mixing and biological conveyor-belt phenomena. Am. J. Sci. 286: 199–238.

Boudreau, B. P., 1997. Diagenetic models and their implementation. Springer-Verlag, Berlin/Heidelberg: 414 pp.

Cochran, J. K., 1985, Particle mixing rates in sediments of the eastern equatorial Pacific: evidence from ^{210}Pb, $^{239,240}Pu$ and ^{137}Cs distributions at MANOP sites. Geochim. Cosmochim. Acta 49: 1195–1210.

Clifton, R. J. ,1991. The use of radionuclides in describing the mixing characteristics of estuarine sediments. In: Kershaw P. J. & D. S. Woodhead (eds), Radionuclides in the Study of Marine Processes), Elsevier Applied Sciences. London 393 pp.

Fisher, J. B., W. J. Lick, P. L. McCall, & J. A. Robbins, 1980. Vertical mixing of lake sediments by tubificid oligochaetes. J. Geophys. Res. 85, C7: 3997–4006.

François, F., J. C. Poggiale, J. P. Durbec & G. Stora, 1997. A new approach for the modelling of sediment reworking induced by a macrobenthic community. Acta Biotheor. 45: 295–319.

Gardner, L. R., P. Sharma & W. S. Moore, 1987, A regeneration model for the effect of bioturbation by fiddler crabs on ^{210}Pb profiles in salt marsh sediments. J. Environ. Rad. 5: 25–36.

Gerino, M., 1990. The effect of bioturbation on particle redistribution in Mediterranean coastal sediment. Preliminary results. Hydrobiologia 207: 251–258.

Gerino, M., G. Stora & J. P. Durbec, 1994. Quantitative estimation of biodiffusive and bioadvective sediment mixing: in situ experimental approach. Oceanol. Acta 17: 547–554.

Gerino, M., R. C. Aller, C. Lee, J. K. Cochran, J. Y. Aller, M. A. Green & D. Hirschberg, 1998. Comparison of different tracers and methods used to quantify bioturbation during a bloom: $^{234}Thorium$, luminophores and chlorophyll a. Estuar. Coast. Shelf Sci. 46: 531–547.

Guinasso, N. L. & D. R. Schink, 1975. Quantitative estimates of biological mixing rates in abyssal sediments. J. Geophys. Res. 80 (21): 3032–3043.

Officer, C. B. & D. R. Lynch, 1982. Interpretation procedures for the determination of sediment parameters from time-dependent flux inputs. Earth Planet. Sci. Lett. 61: 55–62.

Rice, D. L., 1986. Early diagenesis in bioadvective sediments: relationships between the diagenesis of $^{7}beryllium$, sediment reworking rates, and the abundance of conveyor-belt deposit-feeders. J. mar. Res. 44: 149–184.

Smith, J. N., B. P. Boudreau & V. Noshkin, 1986/87. Plutonium and ^{210}Pb distributions in northeast Atlantic sediments: subsurface anomalies caused by non-local mixing. Earth Planet. Sci. Lett. 81: 15–28.

Wheatcroft, R. A., 1992. Experimental tests for particle size-dependent bioturbation in the deep ocean. Limnol. Ocean. 37 (1): 90–104.

Wheatcroft, R. A., P. A. Jumars, C. R. Smith & A. R. M. Nowell, 1990. A mechanistic view of the particulate biodiffusion coefficient: step lenghts, rest period and transport directions. J. mar. Res. 48: 177–207.

Zonta R., L. Zaggia & E. Argese, 1994. Heavy metal and grain-size distribution in estuarine shallow water sediments of the Cona Marsh (Venice Lagoon, Italy). Sci. Total. Environ. 151: 19–28.